Roberts, A. L., "On the Melting of a Semi-Infinite Body Placed in a Warm Stream of Air," *J. Fluid Mech.*, 4, 505 (1958).
Savino, J. M., J. F. Zumdieck, and R. Siegel, "Experimental Study of Freezing and Melting of Flowing Warm Water at a Stagnation Point on a Cold Plate," Fourth Int. Heat Transfer Conference, Paris-Versailles, 1, Cu 2.10 (1970).
Sitharamayya, S., and K. Subba Raju, "Heat Transfer Between an Axisymmetric Jet and a Plate Held Normal to the Flow," *Can. J. Chem. Eng.*, 47, 365 (1969).
Stewart, W. E., and R. Prober, "Heat Transfer and Diffusion in Wedge Flows with Rapid Mass Transfer," *Intern. J. Heat Mass Transfer*, 5, 1149 (1962).
Yang, K. T., "Formation of Ice in Plane Stagnation Flow," *Appl. Sci. Res.*, 17, 377 (1966).
Yen, Y. C., and A. Zehnder, "Melting Heat Transfer with Water Jet," *Intern. J. Heat Mass Transfer*, 16, 219 (1973).

Manuscript received September 26, 1978; revision received February 12 and accepted February 20, 1979.

Flow Through Tubes with Sinusoidal Axial Variations in Diameter

J. A. DEIBER
and
W. R. SCHOWALTER
Department of Chemical Engineering
Princeton University
Princeton, New Jersey 08540

An iteration technique has been developed to solve the equations of motion for flow of an incompressible Newtonian fluid through a circular tube with a radius which varies sinusoidally in the axial direction. The iteration is essentially geometric; one proceeds from a solution for flow through a tube in which the wavelength of diameter change in the axial direction is arbitrarily large to a solution for the wavelength and amplitude of interest. Theoretical predictions of inception of secondary flow are in good agreement with experiments.

SCOPE

Several solutions now exist for flow of Newtonian fluids through tubes with axial periodic variations in diameter. These range from finite-difference solutions of the Navier-Stokes equation for flow through tubes with cusp shaped walls to solutions of the creeping flow equation for flow through tubes with sinusoidally varying diameter. The results are believed to be representative of the flow, under certain conditions, in packed beds and in porous rock. Thus, the work pertains to heat and mass transfer problems in packed beds and to questions associated with secondary and tertiary recovery of petroleum.

It was our desire to provide both computational and experimental results for flow in a circular tube with sinusoidal axial variations in diameter. Chow and Soda (1972) have solved the problem analytically over a limited range of parameters, and Fedkiw and Newman (1977) used a collocation method for the same geometry in the creeping flow regime. The computations presented here remain valid beyond the point where inertial effects are negligible. A new iteration technique was used in which the problem is first solved for a tube wavelength such that locally Poiseuille flow obtains. The wavelength was then decreased by suitably small decrements until a solution was found for the wavelength of interest. The method was found to be economical in terms of computer time.

Experiments were conducted in a tube with an amplitude of radial oscillation equal to 0.3 cm and a wavelength of 6.28 cm. The average tube radius was 1 cm. Pressure drop was measured with conventional pressure taps, and streamlines, including secondary vortices, were observed with a polystyrene latex tracer suspension.

CONCLUSIONS AND SIGNIFICANCE

By iteration from a geometry with a weakly varying axial change in diameter to one in which the change with axial distance is appreciable, one can readily calculate laminar velocity profiles for flow through tubes with variations from the mean diameter which approximate 0.6. Results can be obtained for conditions in which inertial effects are important.

The computations are in good agreement with experimental determinations of friction factor as a function of Reynolds number. The agreement holds beyond the Reynolds number at which inertial effects are important. The shape of a secondary toroidal vortex, which appears as a consequence of inertia, is accurately predicted.

The computational method is attractive because of its relative simplicity and because it can readily be extended to nonlinear equations, such as those which describe the flow of non-Newtonian fluids.

In recent years, there have been several motivations for studying the detailed flow behavior of fluids traversing a conduit in which streamwise variations in cross section are important. For example, Payatakes et al. (1973*a*) have used numerical methods to solve the Navier-Stokes equation for flow in channels formed from packed spheres. Their results were used to provide a better basis for understanding deep-bed filtration (Payatakes et al., 1974). Fedkiw and Newman (1977) modeled mass transfer at high Péclet numbers in a packed-bed reactor. The model was a circular tube with sinusoidally varying diameter in the axial direction. Interest in flow associated aspects of cardiovascular disease led Chow and Soda (1972) to an approximate solution of the full Navier-Stokes equation by an expansion technique. Flow separation following a sinusoidal constriction is described in analysis and experiment by Forrester and Young (1970).

Non-Newtonian flow in tubes with sinusoidal axial variations in diameter can be qualitatively different from the Newtonian counterpart (Dodson et al., 1971). This has led to recognition of the importance of Lagrangian unsteadiness in flow of non-Newtonian fluids through a porous medium (Marshall and Metzner, 1967; James and McLaren, 1975; Savins, 1969; Kemblowski and Dziubinski, 1978). As a step toward our understanding of these flows, we have conducted an experimental and theoretical study of the flow of Newtonian fluids through tubes characterized by radius r_0, where

$$r_0 = a - \epsilon\cos(2\pi\xi/\lambda) \tag{1}$$

Thus ϵ is the amplitude of variation from radius a, along axial distance ξ of a tube. The sinusoidal variation has a wavelength equal to λ.

In prior attempts to solve for the velocity profile and pressure drop in periodically constricted tubes, authors have either (*a*) assumed $\epsilon << a$ or $a << \lambda$ and solved the problem by a perturbation technique (see, for example, Dodson et al., 1971; Burns and Parkes, 1967; Chow and Soda, 1972) or (*b*) converted the equations of motion to finite-difference form and solved the resulting system of equations for given values of the parameters (see, for example, Payatakes et al., 1973*a*, *b*; Azzam and Dullien, 1977; Belinfante, 1962). Also, orthogonal collocation methods have been applied by Neira and Payatakes (1978) and Fedkiw and Newman (1977) when the assumption of slow flow was imposed.

In the work to be presented here we offer a technique which, although iterative in nature, can be conveniently applied to tubes with substantial values of ϵ/a and a/λ. Furthermore, the method has no inherent limitations to linear equations and thus can, in principle, be applied to flows where inertia and/or non-Newtonian effects are important. After demonstrating the procedure, we shall compare the results to data we have obtained in a tube with the configuration described by Equation (1).

FLOW EQUATIONS AND SOLUTION

We express the equations and boundary conditions in dimensionless form. Thus, Equation (1) becomes

$$R_0 = 1 - \alpha\cos Z \tag{2}$$

where $R_0 = r_0/a$, $\alpha = \epsilon/a$, and $Z = 2\pi\xi/\lambda$. Other important dimensionless quantities are $R = r/a$, $\Lambda = 2\pi a/\lambda$, $V = va^2/Q$, and $W = wa^2/Q$. Then, the dimensionless vorticity is

$$\Omega = \frac{\partial W}{\partial R} - \Lambda\frac{\partial V}{\partial Z} \tag{3}$$

and the continuity and vorticity conservation equations are, respectively

$$\frac{1}{R}\frac{\partial}{\partial R}(RV) + \Lambda\frac{\partial W}{\partial Z} = 0 \tag{4}$$

$$Re'\left(W\Lambda\frac{\partial\Omega}{\partial Z} + V\frac{\partial\Omega}{\partial R} - \frac{V}{R}\Omega\right) = \frac{\partial}{\partial R}\left[\frac{1}{R}\frac{\partial}{\partial R}(R\Omega)\right] + \Lambda^2\frac{\partial^2\Omega}{\partial Z^2} \tag{5}$$

where $Re' = Q/(\nu a)$. It is assumed throughout that the flow is axisymmetric and that there is no tangential velocity. Boundary conditions for (4) and (5) are

$$\begin{aligned} &V = W = 0 && \text{at } R = R_0\\ &V = \partial W/\partial R = 0 && \text{at } R = 0\\ &V(R, Z) = V(R, Z + 2\pi), && 0 \le R \le R_0\\ &W(R, Z) = W(R, Z + 2\pi), && 0 \le R \le R_0 \end{aligned} \tag{6}$$

Next we convert from independent variables (R, Z) to corresponding variables (η, Z), where R has been normalized by

$$\eta = R/R_0(\alpha, Z) \tag{7}$$

so that the radial coordinate is $0 \le \eta \le 1$ at all axial positions.

It is convenient to work with the motion equations in terms of the vorticity, defined in Equation (3), and the stream function ψ, defined by

$$W = \frac{1}{R}\frac{\partial\psi}{\partial R} = \frac{1}{\eta R_0^2}\frac{\partial\psi}{\partial\eta} \tag{8}$$

$$V = -\frac{\Lambda}{R}\frac{\partial\psi}{\partial Z} = -\frac{\Lambda}{R_0\eta}\left[\frac{\partial\psi}{\partial Z} - \eta\left(\frac{R_0'}{R_0}\right)\frac{\partial\psi}{\partial\eta}\right]$$

where $R_0' \equiv dR_0/dZ$. Then from Equations (5) and (8) one finds the vorticity conservation equation

$$\begin{aligned} \Lambda Re'\left\{\eta\left(\frac{\partial\psi}{\partial\eta}\frac{\partial\Omega}{\partial Z} - \frac{\partial\psi}{\partial Z}\frac{\partial\Omega}{\partial\eta}\right)\right.&\\ \left. + \left[\frac{\partial\psi}{\partial Z} - \eta\left(\frac{R_0'}{R_0}\right)\frac{\partial\psi}{\partial\eta}\right]\Omega\right\} &= \eta^2\frac{\partial^2\Omega}{\partial\eta^2}[1 + (\Lambda\eta R_0')^2]\\ + \eta\frac{\partial\Omega}{\partial\eta}[1 - (\Lambda\eta)^2(R_0''R_0 - 2R_0'^2)] &+ (\Lambda\eta R_0)^2\frac{\partial^2\Omega}{\partial Z^2}\\ - 2\Lambda^2\eta^3R_0'R_0\frac{\partial^2\Omega}{\partial\eta\partial Z} &- \Omega \end{aligned} \tag{9}$$

From Equations (3) and (8)

$$\begin{aligned} \Omega = \frac{1}{R_0^3\eta^2}\left\{\eta\frac{\partial^2\psi}{\partial\eta^2}[1 + (\Lambda R_0'\eta)^2]\right.&\\ - [1 + (\Lambda\eta)^2(R_0''R_0 - 2R_0'^2)]\frac{\partial\psi}{\partial\eta} + \eta(\Lambda R_0)^2\frac{\partial^2\psi}{\partial Z^2}&\\ \left. - 2R_0'R_0(\eta\Lambda)^2\frac{\partial^2\psi}{\partial Z\partial\eta}\right\} \end{aligned} \tag{10}$$

Setting $\psi = 0$ at $\eta = 0$, one can readily show that

$$\psi = R_0^2\int_0^\eta W\eta'd\eta' \tag{11}$$

and $\psi(\eta = 1) = 1/2\pi$. Thus, boundary conditions for

ψ are

$$\text{at} \quad \eta = 0: \quad \psi = \partial\psi/\partial\eta = 0$$
$$\text{at} \quad \eta = 1: \quad \psi = 1/2\pi; \quad \partial\psi/\partial\eta = 0 \tag{12}$$

and the condition of periodicity requires

$$\psi(\eta, Z) = \psi(\eta, Z + 2\pi), \qquad 0 \leq \eta \leq 1$$
$$\frac{\partial\psi}{\partial Z}(\eta, Z) = \frac{\partial\psi}{\partial Z}(\eta, Z + 2\pi), \quad 0 \leq \eta \leq 1 \tag{13}$$

Then it follows that boundary conditions for Ω are

$$\text{at} \quad \eta = 0: \quad \Omega = 0$$
$$\text{at} \quad \eta = 1: \quad \Omega = \frac{\partial^2\psi}{\partial\eta^2}\frac{(\Lambda R_0')^2 + 1}{R_0^3} \tag{14}$$

and

$$\Omega(\eta, Z) = \Omega(\eta, Z + 2\pi), \quad 0 \leq \eta \leq 1$$

Equations (9) and (10) are solved by rewriting them in finite-difference form and solving by means of an iterative technique. The iteration, however, is an iteration in geometry rather than in values of ψ and Ω at various grid locations. Because the technique is evidently new to this problem, and because it has worked so well, we describe the procedure in some detail. Using central differences for derivatives in η and backward differences for derivatives in Z, one obtains from Equations (9) and (10)

$$A\Omega_{i-1,j} + B\Omega_{i,j} + C\Omega_{i+1,j} = D \tag{15}$$

and

$$A'\psi_{i-1,j} + B'\psi_{i,j} + C'\psi_{i+1,j} = D' \tag{16}$$

where $\psi_{i,j}$ refers to the value of ψ at $\eta = i\Delta\eta$; $Z = j\Delta Z$.

As a base state we consider the solution of Equations (15) and (16) in the limit $\Lambda \to 0$. This corresponds, of course, to a flow which is locally a Poiseuille flow. Thus, we can write

$$\psi^{(0)} = (1 - \eta^2/2)\eta^2/\pi \tag{17}$$
$$\Omega^{(0)} = -4\eta/(\pi R_0^3) \tag{18}$$

and we would expect these results to apply in the limit of an extremely long wavelength for the radius variation given by Equation (1). Now let us consider application of Equations (15) and (16) to a tube with a very small value of Λ (that is, a large wavelength) given by $\Delta\Lambda$. If the increment is sufficiently small, we can find the values of $\psi^{(1)}$ and $\Omega^{(1)}$ corresponding to $\Lambda = \Delta\Lambda$ by substituting $\psi^{(0)}$ and $\Omega^{(0)}$ at appropriate points in Equations (15) and (16). Thus, in general, for $\Lambda = n\Delta\Lambda$ we write

$$\Omega_{i,j}^{(n)} = (1/B)[D^{(n)} - C\Omega_{i+1,j}^{(n-1)} - A\Omega_{i-1,j}^{(n)}] \tag{19}$$

$$\psi_{i,j}^{(n)} = (1/B')[D'^{(n)} - C'\psi_{i+1,j}^{(n-1)} - A'\psi_{i-1,j}^{(n)}] \tag{20}$$

The boundary conditions, Equations (12) through (14), were evaluated at each stage using $\psi_{i,j}^{(n)}$. The value of $\Delta\Lambda$ was chosen to be sufficiently large so that roundoff and truncation errors were not serious problems. $\Delta\Lambda$ was sufficiently small, however, so that at each iteration the periodicity residuals defined as

$$|\psi_{(0,\eta)}^{(n)} - \psi_{(2\pi,\eta)}^{(n+1)}|/\psi_{(0,\eta)}^{(n)}$$
$$|\Omega_{(0,\eta)}^{(n)} - \Omega_{(2\pi,\eta)}^{(n+1)}|/\Omega_{(0,\eta)}^{(n)} \tag{21}$$

were minimized. Typically, the residuals were $o(10^{-3})$.

In general, the grid was constructed by using (21 × 41) points for coordinates η and Z, respectively. The algorithm was used with double precision arithmetic on an IBM 360/91 (Fortran Compiler, Watfiv) computer. Average time of computation was about 20 s. Values of stream function and vorticity were found to be essentially constant over a range of grid sizes. Also, conversion to central-central differences did not have an important effect on the results.

With values of $\psi(\eta, Z)$ and $\Omega(\eta, Z)$ at hand, one can, of course, proceed to compute full velocity profiles. Often, however, less complete information is sufficient. One is especially interested in the effect of diameter variation on pressure drop, and this is conveniently described in terms of a friction factor

$$f = \frac{1}{4}\left(\frac{2a}{\lambda}\right)\frac{\Delta P}{1/2\rho\bar{v}^2} \tag{22}$$

where ΔP is the pressure loss associated with one wavelength of tubing and $\bar{v} = Q/(\pi a^2)$. Then

$$fRe = \int_0^{2\pi}\left\{\Lambda Re' R_0' \eta W\Omega - \eta\Lambda^2 R_0'\left[\frac{\partial\Omega}{\partial Z} - \eta\left(\frac{R_0'}{R_0}\right)\frac{\partial\Omega}{\partial\eta}\right] - V\Omega R_0' + \frac{1}{R_0}\frac{\partial\Omega}{\partial\eta} + \frac{\Omega}{\eta R_0}\right\} dZ \tag{23}$$

where $Re = 2\bar{v}a/\nu$. For smooth tubes ($\alpha = 0$), one obtains the familiar result $fRe = 16$. In the general case ($\alpha \neq 0$), we expect to find $fRe = \text{const}$ if inertial effects are negligible. Equation (23) can be simplified when the condition $\Lambda \to 0$ is introduced; that is, by using $\Omega^{(0)}$ given by Equation (18), one can write

$$fRe = \frac{8}{\pi}\int_0^{2\pi}\frac{dZ}{[R_0(\alpha, Z)]^4} \quad \text{as} \quad \Lambda \to 0 \tag{24}$$

Special care must be taken when comparing friction factors of periodically constricted tubes of different shapes. Even in the particular case $\Lambda \to 0$, Equation (24) shows the possible differences in the value due to the denominator $R_0(\alpha, Z)$.

Results obtained from Equation (23) are shown in Figures 1 and 2. The points labeled S represent inception of flow separation.

COMPARISON WITH PUBLISHED RESULTS

Experiments

Several years ago, Gadəla-Maria (1973) at this laboratory and Porteous (1969) at the University of Delaware performed flow rate-pressure drop experiments in tubes composed of a series of conically shaped converging and diverging sections. Similar experiments were carried out in tubes with nonuniform periodic step changes by Dullien and Azzam (1973) and more recently by Franzen (1977) using the same geometry as Payatakes et al (1973*a*). All of these experiments, despite the differences in tube shape, lead to a common conclusion. A log-log plot of friction factor against Reynolds number is nonlinear beyond a well-defined value of *Re*, which depends on geometrical parameters. Thus, results from nonsinusoidal geometries display the same qualitative features as those of Figures 1 and 2. The experiments of Batra et al. (1970) and of Azzam and Dullien (1977) do not exhibit the same trend. However, the former were conducted in extensible tubes, and the latter were restricted to low values of Reynolds number.

These are the only prior experiments of which the

authors are aware for flow in well-characterized constricted tubes.

Computations

Nonsinusoidal Geometries. Since Payatakes et al. (1973*a*) were interested in flow through arrays of spherical particles, they numerically solved the flow equations for a tube with periodically arranged cusp shaped boundaries. Azzam and Dullien (1977), in a similar fashion, solved the problem for tubes with periodic step changes in diameter. Despite the differences in the shape of these constrictions, the friction factor, at a given value of the Reynolds number, increases with increment in α and Λ in accord with Figures 1 and 2.

Sinusoidal Geometries. Chow and Soda (1972) have performed a regular perturbation of the equations governing fluid motion in a sinusoidal periodically constricted tube. The expansion equations were carried out by using $(\Lambda/2\pi)$ as a small parameter. Although Chow and Soda were primarily interested in energy dissipation, one can readily demonstrate excellent agreement with our results. For example, for $\Lambda \cong 0.63$ and $\alpha \cong 0.3$, their results predict the onset of flow separation at $Re \cong 75$, which is the same as the value shown in Figure 1. However, their equations, which have the advantage of being analytic, are not applicable at values of Re much larger than those at which flow separation occurs. Chow and Soda reported that their solutions should be valid if

$$\frac{Re\alpha\Lambda}{4\pi(1-\alpha^2)^{1/2}} << 1.433 \qquad (25)$$

With a different purpose, Fedkiw and Newman (1977) solved the same problem numerically, but under the assumption of creeping flow. When their Figure 9 is converted to our notation, one finds that for $\alpha > 0.3$, the product fRe decreases slightly with increasing Λ, a trend contrary to that shown in Figure 2.

DESCRIPTION OF EXPERIMENTS

Because of the paucity of experimental data and also as a prelude to study of non-Newtonian behavior in periodically constricted tubes, it was decided to construct a circular conduit with the diameter varying in the flow direction according to Equation (1). Parameters are shown in Table 1.

TABLE 1. DESCRIPTION OF SINUSOIDAL TUBE

a	= 1.0 cm	α	= 0.3
ϵ	= 0.3 cm	L	= 10λ
λ	= 6.28 cm	L_E	= $L/2$
Λ	= 1.0		

The tube was assembled from modules, one of which is shown in Figure 3*a*. Each module was bored from a Plexiglas block with a specially designed tool. Tolerance of the profile is estimated to be ±0.013 cm. A module was joined to its neighbor with O ring seals to form the composite shown in Figure 3*b*. A pressure tap was included in three of the eleven modules constructed. In most cases, either four or eight wavelengths were contained between taps.

Pressure taps were connected to the terminals of a differential pressure transducer of variable reluctance type (Celesco model P90D). The transducer had a range of ±2.54 cm of water and an accuracy of ±½% of full scale. Readings were recorded with a digital electrometer. The transducer was calibrated with a differential pressure applied through two vertical tubes with an appropriate amount of manometric liquid.

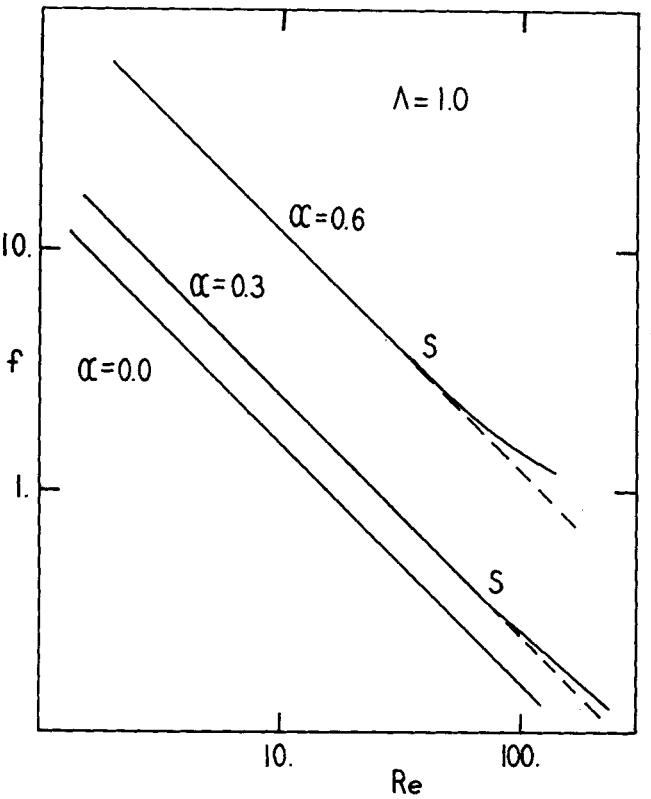

Fig. 1. Friction factor as a function of Reynolds number for a tube with sinusoidally varying diameter. Dashed line indicates a slope of minus one. In this and other figures, S refers to the point at which a toroidal vortex was visible.

Glycerol solutions at different concentrations (32, 48, 60, 68, 75, and 90% by weight) and distilled water were fed to the vertical test section by using either an overhead tank or a pressurized tank, depending on the desired flow rate and the viscosity of the test fluid. The

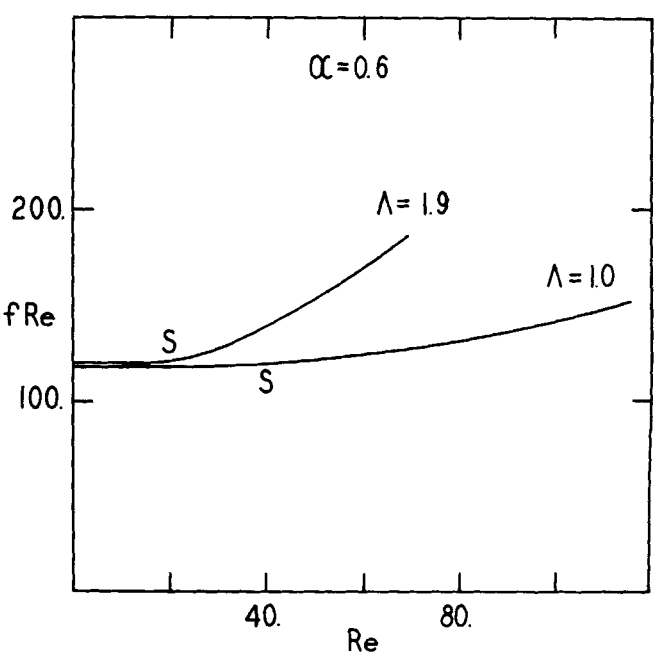

Fig. 2. Effect of wavelength on the relation between friction factor and Reynolds number in a tube with sinusoidally varying diameter.

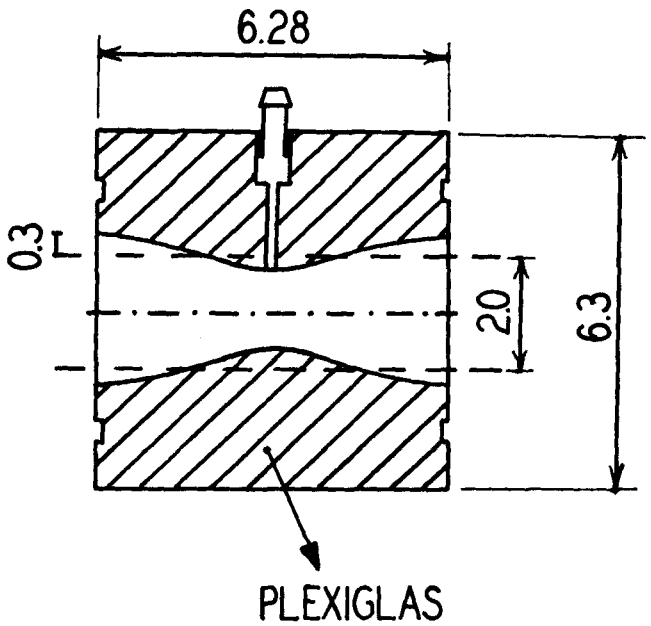

Fig. 3a. Test section module. Dimensions are in centimeters.

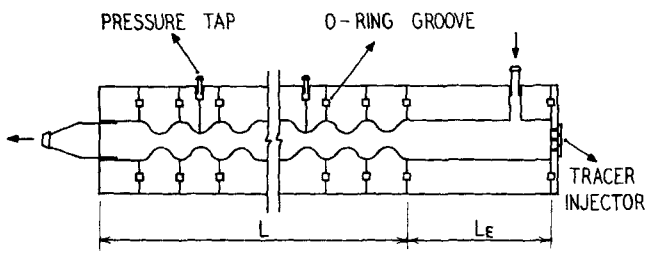

Fig. 3b. Test section assembly.

flow rate was controlled with a set of valves arranged in series and parallel. Flow rate was monitored by measuring the amount of liquid collected in a given period of time.

Glycerol solutions are hygroscopic, and variations in concentration and temperature can produce a significant change in viscosity. Consequently, viscosity was evaluated several times during the course of the experiments, and temperature was monitored at each experimental point.

An important part of the experimental program was flow visualization under conditions for which inertial effects are perceptible. We used 0.5 μm polystyrene spheres for tracer particles. A suspension containing 5 to 10% by volume of spheres was added to the system through a hypodermic needle. The suspension was well dispersed throughout the test section by operating in turbulent flow for a short period of time after introduction of the tracer. The flow rate was then decreased to the desired value. We were able to study the flow patterns by observing the purging of the polystyrene spheres, which gave a milky white appearance in those sections of the flow, such as recirculating vortices, where the particles persisted.

DISCUSSION OF RESULTS

We have already noted that if inertial effects are absent, one should obtain a linear relationship between f and Re^{-1}. This is seen in the computed results shown in Figure 1, where, at low values of the Reynolds number, each of the curves has a slope of minus one. The

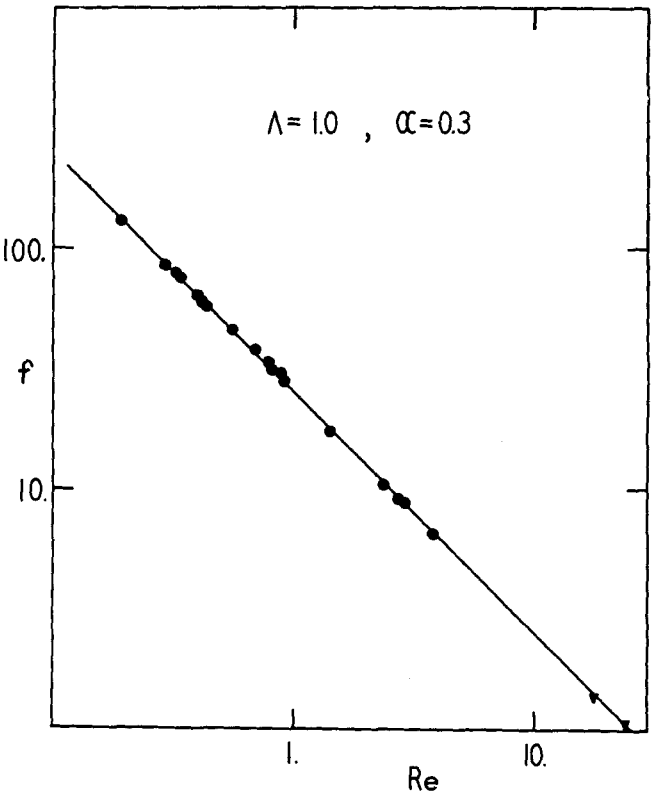

Fig. 4. Comparison of theory and experiment in the creeping flow regime for glycerol-water mixtures. ● refers to 90% glycerol; ▼ to 75 % glycerol.

effects of inertia are also clearly visible, becoming important at lower values of Reynolds number as the amplitude of constriction increases or the wavelength of diameter variation decreases.

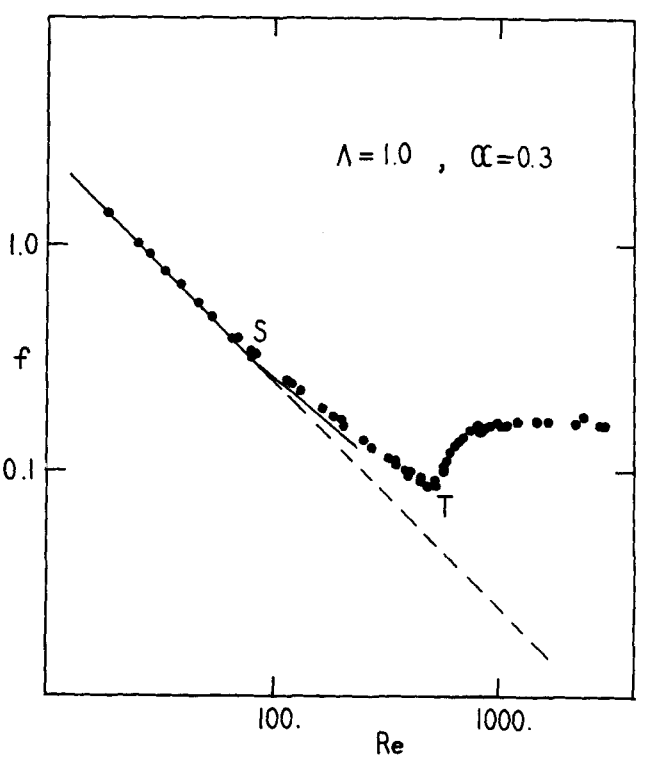

Fig. 5. Comparison of theory and experiment for $\alpha = 0.3$, $\Lambda = 1$. ● are data with concentrations of glycerol ranging from 0 to 68%. At T the system became turbulent, as evidenced by complete mixing of the tracer particles.

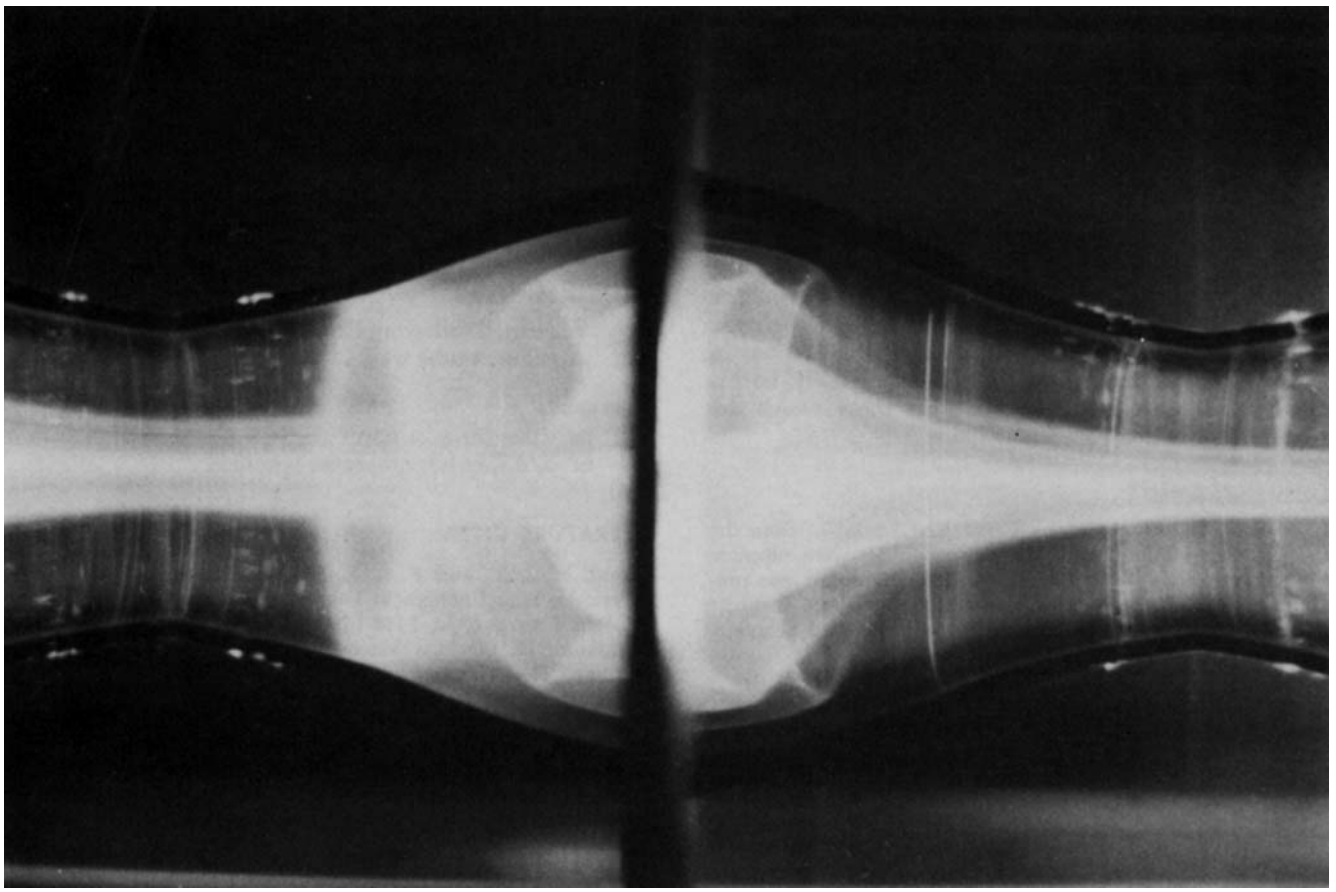

Fig. 6. Photograph of pathlines of tracer particles for $\alpha = 0.3$, $\Lambda = 1$, $Re \cong 242$. Flow is from left to right.

Comparison of computations with experimental results is shown in Figures 4 and 5, which are expanded versions of Figure 1. One notes that in the creeping flow regime, theory and experiment are in excellent agreement, thus validating the experimental technique. Of more importance is the fact that the iteration algorithm used to solve the nonlinear system of Equations (9) and (10) serves as an accurate predictor of the point at which inertial effects become important. Furthermore, departure from the creeping flow result ($f \sim Re^{-1}$) occurs at the Reynolds number ($Re \cong 75$ for the case shown in Figure 5) at which flow separation from the diverging portion of the tube wall and consequent vortex formation is observed from the flow visualization experiments.

Quantitative agreement between theory and experiment decreases as one moves farther into the inertial regime. At present, it is not clear whether this is due to the convergence limits of Equation (21) or to some more basic problem, such as incipient unsteadiness in the flow. A possible source for numerical errors is the linearization, as shown in Equations (15) and (16), of nonlinear terms which are directly related to the magnitude of the Reynolds number.

Although the transition to turbulent flow is always impossible to locate without ambiguity, one can see from Figure 5 that the visual transition point, designated by T, corresponds closely to the abrupt increase in pressure drop which is expected at the transition flow rate.

Finally, it is interesting to compare the structure of the computed and observed secondary flow vortices. In Figure 6 we have shown a photograph of a typical vortex. Somewhat similar separation patterns have been observed by Forrester and Young (1970), who studied flow in a local, but not periodic, contraction-expansion sequence. Note that the vortex in Figure 6 is centered on the diverging portion of the flow, as one would expect. A qualitatively similar secondary flow is shown in Figure 7, where computed streamlines and axial velocity profiles are shown for conditions corresponding to Figure 6.

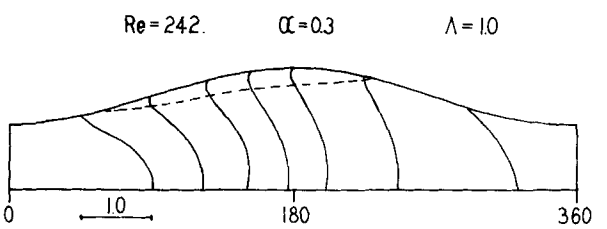

Fig. 7a. Computed shape of axial velocity profile for the conditions of Figure 6.

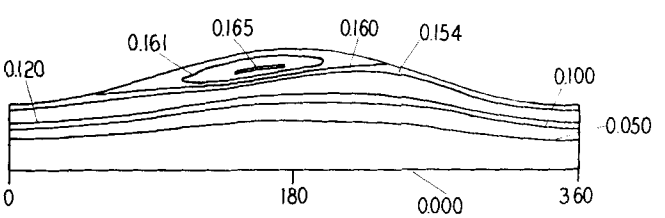

Fig. 7b. Computed streamlines. Conditions are those of Figure 6.

CONCLUSIONS

1. Velocity profiles were computed by an iterative technique in which the shape of a conduit is slowly altered from a reference configuration. With this method one can readily calculate laminar velocity profiles for flow through tubes with substantial variations from the mean diameter. Results can be obtained for conditions in which inertial effects are important.

2. Computations performed as described above are in good agreement with experimental determinations of friction factor as a function of Reynolds number. The flow rate at which inertial effects become important is accurately predicted, as is the shape of a secondary toroidal vortex which appears as a consequence of inertia.

3. The computational method is attractive because of its relative simplicity and because it can readily be extended to nonlinear equations, such as those which describe the flow of non-Newtonian fluids.

ACKNOWLEDGMENT

This work was supported by Grant ENG76-04294 from the National Science Foundation. Helpful comments were supplied by M. A. Neira and A. C. Payatakes. The manuscript was prepared while W. R. Schowalter was at the California Institute of Technology as a Sherman Fairchild Distinguished Scholar.

NOTATION

$A = F_1 - (F_2 - F_6)\Delta\eta/2 - F_4\Delta\eta/(2\Delta Z)$

$A' = G_2 - G_4\Delta\eta/2 - G_5\Delta\eta/(2\Delta Z)$

a = average tube radius

$B = -2F_1 + F_3(\Delta\eta/\Delta Z)^2 - F_5\Delta\eta^2/\Delta Z - F_7\Delta\eta^2 - \Delta\eta^2$

$B' = -2G_2 + G_3(\Delta\eta/\Delta Z)^2$

$C = F_1 + (F_2 - F_6)\Delta\eta/2 + F_4\Delta\eta/(2\Delta Z)$

$C' = G_2 + G_4\Delta\eta/2 + G_5\Delta\eta/(2\Delta Z)$

$D = F_3(2\Omega_{i,j-1} - \Omega_{i,j-2})(\Delta\eta/\Delta Z)^2 + F_4(\Omega_{i+1,j-1} - \Omega_{i-1,j-1})\Delta\eta/(2\Delta Z) - F_5\Omega_{i,j-1}\Delta\eta^2/\Delta Z$

$D' = G_1\Delta\eta^2 + G_3(2\psi_{i,j-1} - \psi_{i,j-2})(\Delta\eta/\Delta Z)^2 + G_5(\psi_{i+1,j-1} - \psi_{i-1,j-1})\Delta\eta/(2\Delta Z)$

$F_1 = \eta^2[1 + (\Lambda\eta R_0')^2]$

$F_2 = \eta[1 - (\Lambda\eta)^2(R_0''R_0 - 2R_0'^2)]$

$F_3 = (\Lambda\eta R_0)^2$

$F_4 = -2\Lambda^2\eta^3 R_0 R_0'$

$F_5 = Re'\Lambda\eta\,\partial\psi/\partial\eta$

$F_6 = -Re'\Lambda\eta\,\partial\psi/\partial Z$

$F_7 = Re'\Lambda\left[\frac{\partial\psi}{\partial Z} - \eta\left(\frac{R_0'}{R_0}\right)\frac{\partial\psi}{\partial\eta}\right]$

f = friction factor, defined in Equation (22)

$G_1 = R_0^3\eta^2\Omega$

$G_2 = \eta(1 + (R_0'\eta\Lambda)^2)$

$G_3 = (\Lambda R_0)^2\eta$

$G_4 = -[1 + (\Lambda\eta)^2(R_0''R_0 - 2R_0'^2)]$

$G_5 = 2R_0'R_0(\eta\Lambda)^2$

L = length of test and exit sections (see Figure 3*b*)

L_E = length of entry section (see Figure 3*b*)

P = pressure, where ΔP is the pressure loss over one wavelength of tubing

Q = volumetric flow rate

$R = r/a$

r = radial coordinate

Re = Reynolds number $= 2\bar{v}a/\nu$

Re' = modified Reynolds number $= Q/(\nu a)$

$V = va^2/Q$

v = radial velocity

$\bar{v} = Q/(\pi a^2)$

$W = wa^2/Q$

w = axial velocity

$Z = 2\pi\xi/\lambda$

Greek Letters

$\alpha = \epsilon/a$

ϵ = amplitude of radius variation [Equation (1)]

$\eta = R/R_0$

$\Lambda = 2\pi a/\lambda$

λ = wave length of radius variation [Equation (1)]

ν = kinematic viscosity (length)^2/time

ξ = axial coordinate

ρ = density

ψ = stream function, defined by Equations (8) and (11)

Ω = vorticity, defined by Equation (3)

Subscripts

i, j = defined following Equation (16)

0 = value at tube wall

Superscripts

(n) = value for $\Lambda = n\Delta\Lambda$

$'$ = d/dZ, unless otherwise specified

LITERATURE CITED

Azzam, M. I. S., and F. A. L. Dullien, "Flow in Tubes with Periodic Step Changes in Diameter: A Numerical Solution," *Chem. Eng. Sci.*, **32**, 1445 (1977).

Belinfante, D. C., "On Viscous Flow in Pipe with Constrictions," *Proc. Camb. Phil. Soc.*, **55**, 405 (1962).

Batra, V. K., G. D. Fulford, and F. A. L. Dullien, "Laminar Flow through Periodically Convergent-Divergent Tubes and Channels," *Can. J. Chem. Eng.*, **48**, 622 (1970).

Burns, J. C., and T. Parkes, "Peristaltic Motion," *J. Fluid Mech.*, **29**, 731 (1967).

Chow, J. C. F., and K. Soda, "Laminar Flow in Tubes with Constriction," *Phys. Fluids*, **15**, 1700 (1972).

Dodson, A. G., P. Townsend, and K. Walters, "On the Flow of Newtonian and Non-Newtonian Liquids through Corrugated Pipes," *Rheol. Acta*, **10**, 508 (1971).

Dullien, F. A. L., and M. I. S. Azzam, "Flow Rate-Pressure Gradient Measurements in Periodically Nonuniform Capillary Tubes," *AIChE J.*, **19**, 222 (1973).

Fedkiw, P., and J. Newman, "Mass Transfer at High Péclet Numbers for Creeping Flow in a Packed-Bed Reactor," *ibid.*, **23**, 255 (1977).

Forrester, J. H., and D. F. Young, "Flow through a Converging-Diverging Tube and its Implications in Occlusive Vascular Disease. Parts I and II," *J. Biomechanics*, **3**, 297, 307 (1970).

Franzen, P., "Strömungskanal mit veränderlichem Kreisquerschnitt als Modell für Zufallsschüttungen gleich grosser Kugeln," *Rheol. Acta*, **16**, 548 (1977).

Gadala-Maria, F., "The Study of a Model for the Flow of Viscoelastic Fluids through Porous Media," Department of Chemical Engineering, Princeton Univ., N.J. (1973).

James, D. F., and D. R. McLaren, "The Laminar Flow of Dilute Polymer Solutions through Porous Media," *J. Fluid Mech.*, **70**, 733 (1975).

Kemblowski, Z., and M. Dziubiński, "Resistance to Flow of Molten Polymers through Granular Beds," *Rheol. Acta*, **17**, 176 (1978).

Marshall, R. J., and A. B. Metzner, "Flow of Viscoelastic Fluids through Porous Media," *Ind. Eng. Chem. Fundamentals*, **6**, 393 (1967).

Neira, M. A., and A. C. Payatakes, "Collocation Solution of Creeping Newtonian Flow through Periodically Constricted Tubes with Piecewise Continuous Wall Profile," *AIChE J.*, **24**, 43 (1978).

Payatakes, A. C., Chi Tien, and R. M. Turian, "Numerical Solution of Steady State Incompressible Newtonian Flow through Periodically Constricted Tubes," *ibid.*, **19**, 67 (1973*a*).

———, "Further Work on the Flow through Periodically Constricted Tubes—A Reply," *ibid.*, 1036 (1973*b*).

———, "Trajectory Calculation of Particle Deposition in Deep Bed Filtration Part I. Model Formulation," *ibid.*, **20**, 889 (1974).

Porteous, K. C., "The Behavior of Dilute Viscoelastic Liquids under High Deborah Number Conditions," M.S. thesis, Department of Chemical Engineering, Univ. Del., Newark (1969).

Savins, J. G., "Non-Newtonian Flow through Porous Media," *Ind. Eng. Chem.*, 61, 18 (1969).

Manuscript received October 10, 1978; revision received March 1, and accepted March 25, 1979.

Vapor-Liquid Equilibrium

H. C. VAN NESS

and

M. M. ABBOTT

Department of Chemical and Environmental Engineering
Rensselaer Polytechnic Institute
Troy, New York 12181

A general treatment of fugacities of liquid mixtures yields the proper thermodynamic functions for dealing with nonidealities of liquid phases in equilibrium with vapor mixtures for systems containing supercritical components. The activity coefficients of the supercritical components may be based on standard state fugacities for the hypothetical pure liquids or on Henry's constants. A comparison of the rigorous thermodynamic equations which apply to the liquid phase for the two alternatives shows that they are equivalent.

Part VI. Standard State Fugacities for Supercritical Components

SCOPE

Vapor/liquid equilibrium calculations for systems which include one or more supercritical components (that is, species whose critical temperatures are below the system temperature) are complicated by the fact that these species do not exist as pure liquids at the temperature of the system. Thus one cannot know the vapor pressure or, more fundamentally, the fugacity of the pure liquid upon which the activity coefficient is usually based. Moreover, high pressures are characteristic of such systems, and the usual assumption of pressure independence of the activity coefficients is not satisfactory.

For a supercritical component, two standard state fugacities upon which to base the activity coefficient have been used: first, a value obtained by extrapolation for the hypothetical pure liquid, and second, the value of Henry's constant. The latter has been considered preferable because it can be measured. For binary systems, little difficulty is encountered with the thermodynamic treatment in either case. For multicomponent systems, however, there has been much confusion.

A general treatment is presented here which yields the proper thermodynamic relations for both choices of standard state fugacity. The derivation of appropriate equations for activity coefficients is straightforward, progressing from binary through ternary to multicomponent systems.

CONCLUSIONS AND SIGNIFICANCE

The standard state fugacities for supercritical components of systems in vapor/liquid equilibrium may equally well be taken as Henry's constants or as the fugacities of hypothetical pure liquids. The thermodynamic treatment of liquid phase nonidealities based on activity coefficients for the two cases yields equivalent results. However, use of Henry's constants leads, in practice, to complex equations. The method of Prausnitz and Chueh (1968) as corrected by Abrams et al. (1975) is an example, but it incorporates additional and unnecessary complexity. Activity coefficients based on fugacities of the hypothetical pure liquids as standard state values lead to far simpler equations and have the additional advantage of symmetry. For a supercritical component, fugacities for the standard state of hypothetical pure liquid are as readily determined as are Henry's constants.

With the thermodynamics on a firm theoretical foundation, it becomes clear that treatment through activity coefficients of vapor/liquid equilibria in systems containing supercritical components is severely limited by our inability to take properly into account the effect of pressure on the activity coefficients and to model their composition dependence.